BASIC SCIENCE

Nanomedicine: Nanotechnology, Biology, and Medicine
14 (2018) 35–45

Original Article

nanomedjournal.com

Gold nanoparticles in injectable calcium phosphate cement enhance osteogenic differentiation of human dental pulp stem cells

Yang Xia, MD[a,b,c], Huimin Chen[b], Feimin Zhang, MD[b], Chongyun Bao, MD[c,d], Michael D. Weir, PhD[c], Mark A. Reynolds, MD[c], Junqing Ma, MD[b], Ning Gu, PhD[a,e,*], Hockin H.K. Xu, PhD[c,f,g,**]

[a]*Jiangsu Key Laboratory for Biomaterials and Devices, School of Biological Science and Medical Engineering, Southeast University, Nanjing, Jiangsu, China*
[b]*Jiangsu Key Laboratory of Oral Diseases, Nanjing Medical University, Nanjing, Jiangsu, China*
[c]*Department of Advanced Oral Sciences & Therapeutics, University of Maryland School of Dentistry, Baltimore, MD, USA*
[d]*State Key Laboratory of Oral Diseases, West China Hospital of Stomatology, Sichuan University, Chengdu, Sichuan, China*
[e]*Collaborative Innovation Center of Suzhou Nano Science and Technology, Suzhou, Jiangsu, China*
[f]*Center for Stem Cell Biology and Regenerative Medicine, University of Maryland School of Medicine, Baltimore, MD, USA*
[g]*University of Maryland Marlene and Stewart Greenebaum Cancer Center, University of Maryland School of Medicine, Baltimore, MD, USA*

Received 29 April 2017; accepted 15 August 2017

Abstract

In this study, a novel calcium phosphate cement containing gold nanoparticles (GNP-CPC) was developed. Its osteogenic induction ability on human dental pulp stem cells (hDPSCs) was investigated for the first time. The incorporation of GNPs improved hDPSCs behavior on CPC, including better cell adhesion (about 2-fold increase in cell spreading) and proliferation, and enhanced osteogenic differentiation (about 2–3-fold increase at 14 days). GNPs endow CPC with micro-nano-structure, thus improving surface properties for cell adhesion and subsequent behaviors. In addition, GNPs released from GNP-CPC were internalized by hDPSCs, as verified by transmission electron microscopy (TEM), thus enhancing cell functions. The culture media containing GNPs enhanced the cellular activities of hDPSCs. This result was consistent with and supported the osteogenic induction results of GNP-CPC. In conclusion, GNP-CPC significantly enhanced the osteogenic functions of hDPSCs. GNPs are promising to modify CPC with nanotopography and work as bioactive additives thus enhance bone regeneration.

Key words: Gold nanoparticles; Nanoparticle internalization; Calcium phosphate cement; Dental pulp stem cells; Bone tissue engineering

Bone defects arise from skeletal diseases, congenital malformations, trauma, and tumor resections and require bone reconstruction.[1-3] Calcium phosphate cements are promising bone substitutes with excellent bioactivity, biocompatibility and osteoconductivity.[4,5] These materials stand out as injectable bone cements owing to their self-setting and in situ hardening capabilities.[6,7] The first calcium phosphate cement approved by the Food and Drug Administration (FDA) was based on tetracalcium phosphate [TTCP: $Ca_4(PO_4)_2O$] and dicalcium phosphate anhydrous [DCPA: $CaHPO_4$] (referred to as CPC).[7] In addition, several other calcium phosphate cements were developed with different compositions.[5,8]

The authors claim that there is no conflict of interest: This study was supported by the National Institutes of Health [Grant number R01 DE14190 and R21 DE22625], National Natural Science Foundation of China [Grant number 81400486 and 81371179], Natural Science Foundation of Jiangsu [Grant number BK20140911 and BK20150048], Postdoctoral Foundation of Jiangsu [Grant number 1402044B], China Postdoctoral Foundation [Grant number 2015M571647], Project Funded by the Priority Academic Program Development of Jiangsu Higher Education Institutions [Grant number 2014-37], National Key Research Project [Grant number 2016YFA0201704/2016YFA0201700], Jiangsu Scholarship for Overseas Studies [Grant number JS-2014-065], Jiangsu Medical Youth Talent [QNRC2016853], and University of Maryland School of Dentistry bridge fund.

* Correspondence to: N. Gu, Jiangsu Key Laboratory for Biomaterials and Devices, School of Biological Science and Medical Engineering, Southeast University, Nanjing, Jiangsu 210096, China.

** Correspondence to: H.H.K. Xu, Biomaterials and Tissue Engineering Division, Department of Advanced Oral Sciences & Therapeutics, University of Maryland School of Dentistry, Baltimore, MD 21201, USA.

E-mail addresses: guning@seu.edu.cn (N. Gu), hxu@umaryland.edu (H.H.K. Xu).

https://doi.org/10.1016/j.nano.2017.08.014
1549-9634/

Macroporous CPC was developed with injectability, good mechanical properties and the ability to encapsulate stem cells.[9-11] Its injectability is suitable for minimally-invasive procedures and filling defects with complex shapes. Its moldability enables surgical treatments customized to the shape of the targeted defects, especially for achieving esthetics in dental and craniofacial areas. Recently, material-based, biochemical, and physical science-based approaches have emerged as novel approaches to modify the cells.[12] Efforts were made to improve the osteogenic properties of CPC by incorporating bioactive agents to stimulate cellular actions for rapid bone healing and regeneration.[13] Hybrid materials were investigated, including the incorporation of drugs,[14] growth factors[15] and nanoparticles.[16] Nano-materials are promising additives to CPC to enhance mechanical properties and biocompatibility. So far, nanoparticles including silicon carbide (SiC), titanium dioxide (TiO_2) and silica (SiO_2), and nanofibers such as carbon nanotubes have been incorporated into CPC, showing improvements in the physico-chemical and mechanical properties.[17]

Nanomaterials can be incorporated into CPCs via either powder or liquid forms. The liquid method could potentially achieve a better dispersion of the nanoparticles than the powder form where agglomeration of nanoparticles is a challenge. A literature search revealed no report on gold nanoparticles (GNPs) in a solution form incorporated into calcium phosphate cements.

GNPs are attractive due to their unique physical and chemical properties.[18,19] They have many prominent advantages such as excellent biocompatibility, facile synthesis method and versatile surface functionalization.[20] Indeed, GNPs have been developed as a new generation of osteogenic agents for bone tissue regeneration.[21,22] They can promote osteogenic differentiation and inhibit adipogenic differentiation of mouse mesenchymal stem cells (MSCs) through the p38 mitogen-activated protein kinase (MAPK) pathway.[21] In another study, osteogenic differentiation of human adipose-derived stem cells (ADSCs) was sensitive to the particle size of GNPs.[23] GNPs inhibited the receptor activator of the nuclear factor-κb ligand pathway towards osteoclast formation in bone marrow-derived macrophages.[24] However, GNPs did not affect the osteogenesis of MG63 osteoblast-like cells.[25]

Stem cells are another important aspect in tissue engineering.[26] Human dental pulp stem cells (hDPSCs) are postnatal stem cells with similar gene expression profiles and differentiation capability to those of bone marrow stromal cells (BMSCs).[27] hDPSCs can be induced and differentiated into odontoblast-like and osteoblast-like cells by a variety of inducing reagents such as dexamethasone (Dex), β-glycerophosphate (β-GP) and 1,25-dihydroxyvitamin D, to help repair dentin and bone after injury.[28] In addition, hDPSCs have extensive differentiation ability and can attach to biomaterials, which makes them ideal for tissue reconstruction.[29] Furthermore, the association of hDPSCs with appropriate physiological osteogenic scaffold is a promising approach in healing of large craniofacial bone defects in vivo.[30]

Accordingly, the objectives of this study were to incorporate a GNP solution into the CPC paste, to develop a novel GNP-CPC scaffold, and to investigate the osteogenic differentiation of hDPSCs seeded on GNP-CPC scaffold for bone tissue engineering for the first time. The following hypotheses were tested: (1) The addition of GNPs would improve the properties of CPC; (2) The osteogenic differentiation of hDPSCs would be enhanced via GNP incorporation in CPC; (3) The GNP incorporation would change the microstructure of CPC which would contribute to improving cell adhesion, spreading and osteogenic differentiation.

Methods

Preparation of CPC powder

The CPC powder consisted of TTCP and DCPA. TTCP was synthesized from a solid-state reaction between DCPA and $CaCO_3$, then ground in a blender to obtain particle sizes of 1–80 μm (median = 5 μm). DCPA was ground to obtain particle sizes of 0.4–3.0 μm (median = 1.0 μm). TTCP and DCPA were mixed at a molar ratio of 1:3 to form the CPC powder.

Preparation and characterization of GNPs

Gold (III) chloride trihydrate, sodium citrate tribasic dihydrate (Sigma-Aldrich, MO, USA) was used as-received. The fabrication method was described elsewhere.[31] Briefly, 95 mL of ultrapure deionized water and 1 mL of 1% chloroauric acid trihydrate was added to a 250-mL three-necked flask. The solution was heated to its boiling point. Then, 4 mL of 1% sodium citrate was added to the solution. The mixture was heated for another 25 min and subsequently cooled down to room temperature. During this process, stirring was maintained. Finally, the whole volume of colloidal suspension was calibrated to 100 mL. This stable colloidal suspension was concentrated ten times by centrifugation at 10,000 rpm for 33 min to achieve the final gold concentration in water of 0.5 mg/mL. The nanoparticle morphology in this homogenous and monodispersed nanosolution was examined by transmission electron microscope (TEM; JEOL-7100, MA, USA). The hydrodynamic diameters of used nanoparticles were measured by dynamic light scattering (DLS) with a particle size analyzer (Malvern Zetasizer Nano ZS90, Malvern, UK). The as-fabricated citrate-stabilized GNPs were used for subsequent experiments.

Preparation of GNP-CPC scaffold

Either water or the GNPs solution was used as the CPC liquid to mix with CPC powder. The powder to liquid ratio was 2:1. The fabrication process was illustrated in Figure 1. Two groups were made:

(1) CPC control: CPC powder mixed with distilled water;
(2) GNP-CPC: CPC powder mixed with GNP solution;

Characterization of GNP-CPC scaffold

Scanning electron microscope

Specimens were set in a water bath at 37 °C for 1 day. Scanning electron microscopy (SEM, JEOL JSM-840, MA, USA) was used to investigate the microstructure of the GNP-CPC scaffold. Samples were sputter-coated with platinum before examination.

Mechanical properties

Molds of 3 × 4 × 25 mm were used to make specimens. The specimens were sandwiched between two glass slides and set in 37 °C water bath for 4 h, then demolded and immersed in 37 °C

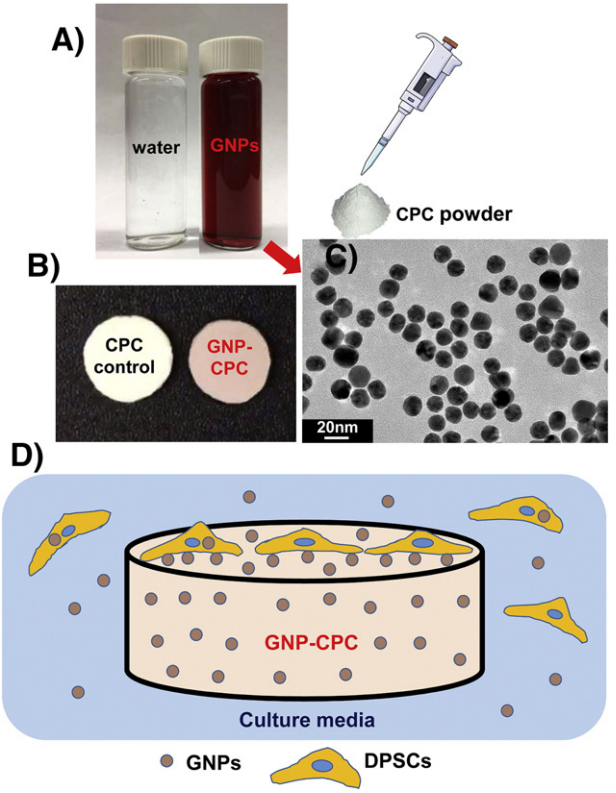

Figure 1. Schematic of the fabrication procedure for GNP-CPC. (A) CPC liquid used. (B) As fabricated scaffolds. (C) TEM image of GNPs. (D) Possible ways of cells affected by GNP-CPC.

water for 20 h. A standard three-point flexural test with a span of 20 mm was used at a crosshead speed of 1 mm/min on a computer-controlled Universal Testing Machine (model 5500R, Instron, Canton, MA). Flexural strength $S = 3F_{max}L/(2bh^2)$, where F_{max} is the maximum load on the load–displacement (F-d) curve, L is span, b is specimen width, and h is thickness. Elastic modulus $E = (F/d)\ (L^3/[4bh^3])$, where load F divided by displacement d is the slope of the load–displacement curve.

Powder x-ray diffraction (XRD) analysis of GNP-CPC scaffold

The phase composition in GNP-CPC was evaluated via XRD with Ni-filtered Cu Kα radiation. Step-scanning was performed at an integration time of 50 s with intervals of 0.02° (2θ). Peak indexing was carried out by means of ICSD 22059 for hydroxyapatite (HA), and ICSD 52249 for gold.

In vitro degradation and gold element release from GNP-CPC scaffold

In vitro degradation was tested following a previous method.[32] Briefly, the samples were prepared in molds with 6 mm in diameter and 1 mm in thickness. After immersion in water for 1 d, the samples were dried and weighed. Then, after soaking in a demineralizing solution (1.15 mmol/L Ca, 1.2 mmol/L P, 133 mmol/L NaCl, pH adjusted to 3–5 by adding HCl or NaOH) for a certain time, the samples were taken out, dried again and weighed. At a pH of 7.4, HA is the least soluble of the naturally occurring calcium phosphate salts.[33] Thus, pH 4 and pH 5.5 solutions were used for the in vitro degradation test, to simulate resorption by osteoclasts via low pH. The mass loss of each sample was calculated as: Mass loss = (Sample weight before immersion − Sample weight after immersion) / Sample weight before immersion.

Table 1
Real-Time Polymerase Chain Reaction Primers Used in This Study.

Gene	Primer Sequence
GAPDH	Forward: 5′-GCACCGTCAAGGCTGAGAAC-3′
	Reverse: 5′-TGGTGAAGACGCCAGTGGA-3′
ALP	Forward: 5′-CCTTGTAGCCAGGCCCATTG-3′
	Reverse: 5′-GGACCATTCCCACGTCTTCAC-3′
COL Iα	Forward: 5′-AAGAGGCGAGAGAGGTTTCC-3′
	Reverse: 5′-ACCAGCATCACCCTTAGCAC-3′
RUNX2	Forward: 5′-ACCTTGACCATAACCGTCTTCAC-3′
	Reverse: 5′-TCCCGAGGTCCATCTACTGTAAC-3′
OCN	Forward: 5′- AGAGCCCTCACACTCCTCGC-3′
	Reverse: 5′-TGCACCTTTGCTGGACTCTGC-3′
OPN	Forward: 5′-TGTGGTTTATGGACTGAGGTCAA-3′
	Reverse: 5′-TGGCCTTGTATGCACCATTC-3′

The gold element release was evaluated by immersing the GNP-CPC samples in 1 × PBS for 4 weeks. The amount of gold element release vs. time was determined by atomic absorption spectroscopy (AAS, 180–80, Hitachi, Japan).

Water contact angle

The surface energy of CPC control and GNP-CPC scaffolds was examined by measuring contact angles using the sessile drop technique with a contact angle meter[34] (JC2000C2, Shanghai Zhongchen Powereach Company, China). The liquids used for the experiments were distilled water and neutral red solution (Sigma-Aldrich). Water spreading area was calculated by Image-Pro Plus 6.0 software (Media Cybernetics, MD, USA).

Protein adsorption test

To examine whether GNP incorporation in CPC would change the protein adsorption, protein adsorption onto CPC control and GNP-CPC scaffolds was determined.[35] Each disk sample (6 mm in diameter and 1 mm in thickness) was immersed in PBS for 2 h. The samples then were immersed in a bovine serum albumin (BSA) (Sigma-Aldrich) solution at 37 °C for 12 h, which contained BSA at a concentration of 4.5 g/L. The disks then rinsed with fresh PBS, immersed in 1% sodium dodecyl sulfate (SDS)/PBS solution, and sonicated at room temperature for 20 min to completely detach the BSA from disk surfaces. A protein analysis kit (Pierce™ Coomassie, Bradford, Thermo Fisher Scientific, Pittsburgh, PA, USA) was used to determine the BSA amount adsorbed onto the sample.

In vitro cell assay on scaffolds

Isolation and culture of hDPSCs

The isolation and culture of hDPSCs were approved by the University of Maryland Baltimore Institutional Review Board, and followed the procedures reported previously.[11] Briefly, pulp tissues were minced and digested in a solution of 3 mg/mL of collagenase type I and 4 mg/mL dispase for 30–60 min at 37 °C. Cell suspension was obtained by passing the digested tissue through a 70-μm cell strainer. The cells were pelleted and seeded in culture dishes, and incubated with DMEM growth medium

Table 2
Main parameters of the used gold nanoparticles.

Sample	Hydrodynamic size (nm)	Polydispersity index (PDI)	Zeta potential
Au	23.80 ± 3.68	0.243 ± 0.06	−26.63 ± 1.74

(DMEM +10% fetal calf serum +1% penicillin streptomycin, Gibco) in a humidified atmosphere of 95% air and 5% CO_2. Non-adherent cells were removed 48 h after the initial plating. The medium was replaced every 3 d. The cells were tested to confirm the expression of CD29, CD44, CD166, CD73 which are the surface characteristic markers of mesenchymal stem cells (MSCs), and the negative expressions of CD34, CD45, CD14 which are typical for hematopoietic cells. The 4th passage hDPSCs were used in the following experiments.

Cell adhesion and spreading

hDPSCs were seeded on GNP-CPC, using those on CPC as control. The culture medium was used in adhesion and proliferation tests; the osteogenic medium was used in osteogenic assay. Cell imaging on the scaffolds after seeding at predetermined time-points was performed by immersing the scaffold in a live/dead staining solution (Invitrogen, CA, USA). The cells were examined via epifluorescence microscopy (Eclipse TE-2000S, Nikon, Tokyo, Japan). Three images were taken at random locations for each sample, with 6 samples yielding 18 images for each scaffold at each time point. The images were analyzed by Image-Pro Plus 6.0 software. Live cell spreading area was calculated as: $S = S_{total} / N_{Live}$, where S_{total} is the total cell spreading area on the image, and N_{Live} is the number of live cells. A cell counting kit (CCK-8, Enzo Biochem, Inc., New York, USA) was used to evaluate the adhered cell ratio normalized by the culture well control at 4 h after seeding. Cell adhesion ratio = OD value of scaffold group / OD value of culture well control.[36]

Cell proliferation

The same CCK-8 kit was used to evaluate cell proliferation at 1, 4, 7 and 14 days. After incubate in dark for 2 h, an optical density of 450 nm (OD_{450nm}) was detected using a microplate reader (SpectraMax M5, Molecular Devices, CA, USA).

Osteogenic differentiation

Alkaline phosphatase activity (ALP)

At 4, 7 and 14 days, cells were lysed and assayed for ALP activity using a fluorometric ab83371 Alkaline Phosphatase Assay kit (Abcam, CA, USA). ALP activity was normalized by total protein of each sample which was quantified using a Pierce BCA Protein Assay Kit (Thermo Fisher Scientific, MA, USA).

Quantitative reverse transcription–polymerase chain reaction (qRT-PCR)

qRT-PCR was used to examine the expression of osteogenic differentiation marker genes. These genes included ALP, collagen type Iα (COLIα), runt-related transcription factor 2 (RUNX2), and osteocalcin (OCN). Glyceraldehyde 3-phosphate dehydrogenase (GAPDH) was used as the housekeeping gene. Primer sequences for the aforementioned genes are listed in Table 1. Relative expression was evaluated using the $2^{-\Delta\Delta Ct}$ method and normalized by the C_t of the housekeeping gene GAPDH. C_t of hDPSCs cultured on CPCs served as their own calibrator at each determined test time point.

Mineral synthesis by hDPSCs on scaffolds

At predetermined time-points, the scaffolds were stained with 2% Alizarin Red S (ARS, Millipore, Billerica, MA, USA), which stained calcium-rich deposits made by the cells into a dark red color. Quantification of the mineralized rate was performed by measuring the absorbance at 550 nm after eluting the ARS deposit with 10% cetylpyridinium chloride (Sigma-Aldrich, MO, USA).[37] The amount of synthesized minerals on CPCs served as their own calibrator at each determined test time point.

Detection of GNP uptake inside the hDPSCs

To detect whether there were GNPs internalized by hDPSCs, cell samples were prepared at 7 days after seeding. They were observed by TEM (Tecnai™ G2 Spirit Twin system, FEI, Hillsboro, OR, USA) to detect GNPs inside the individual cell. Quantitative measurement of gold content inside the cells was done by Inductively Coupled Plasma Optical Emission Spectrometry (ICP-OES, Optima 5300DV, PerkinElmer, MA, USA).

In vitro cellular behavior in GNPs medium

To detect the effects of GNPs alone on cells without CPC scaffolds, hDPSCs were cultured in media supplemented with 5 ppm GNPs, using media without GNPs as control. Cell proliferation on tissue culture polystyrene (TCPS) and osteogenic differentiation including ALP activity, osteogenic gene expressions, and mineral synthesis by the cells were measured.

Statistical analysis

All data were expressed as mean value and standard deviation (SD). A SPSS statistical package (version 22.0; IBM Corp., Armonk, New York, USA) was used for the statistical analysis. Group comparisons were conducted by one-way ANOVA with Bonferroni *post-hoc* tests. Differences were considered significant if $p < 0.05$ and highly significant if $p < 0.01$.

Results

Characterization of GNPs and GNP-CPC

The fabrication schematic of GNP-CPC is illustrated in Figure 1. GNPs were in the clear red solution (Figure 1, *A*). GNP-CPC had a pink color, while CPC control was white (Figure 1, *B*). When examined by TEM, GNPs were well dispersed and homogenous in size with an average of 18 nm in diameter (Figure 1, *C*). The main parameters of GNPs measured by Malvern Zetasizer Nano ZS90 are listed in Table 2. The GNPs are low in polydispersity index (PDI), indicating a narrow size distribution.

Surface morphology of the scaffolds was examined by SEM. Both scaffolds had many particulates which consisted of small crystallites (Figure 2, *A* and *B*). The incorporation of GNPs

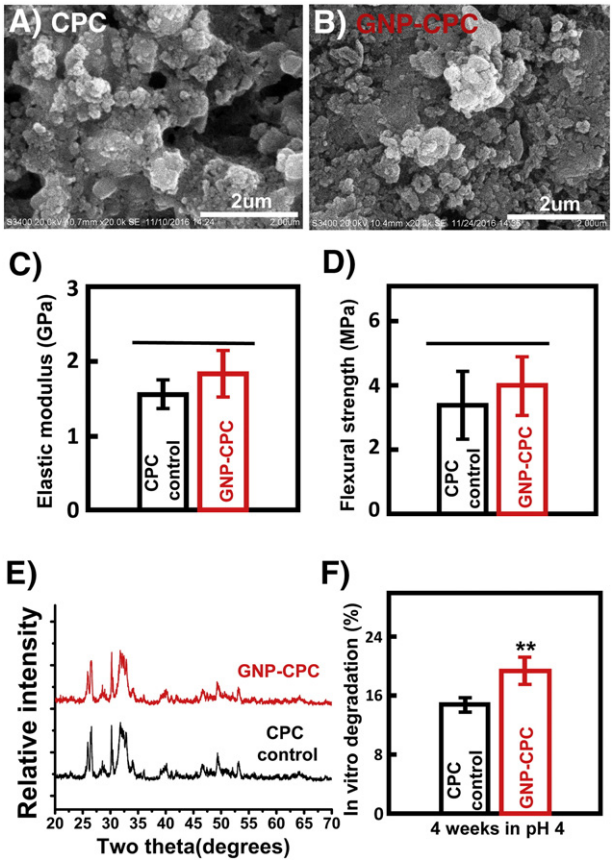

Figure 2. Structural, physical and mechanical properties of GNP-CPC and CPC. (A) and (B) Surface microstructure. (C) Elastic modulus. (D) Flexural strength. (E) X-ray diffraction patterns. (F) In vitro degradation in pH 4 physiological solution. ($n = 9$). (**, represents $p < 0.01$).

appeared to decrease the crystal size of the scaffold, showing a finer microstructure in b than in a. EDS was done to detect surface elements of GNP-CPC (Figure S1), but gold was not detected. GNPs incorporation did not change the mechanical properties; elastic modulus and flexural strength was similar for both scaffolds ($p > 0.05$, Figure 2, *C* and *D*). XRD was used to detect the composition of GNP-CPC, with no new peaks detected compared with CPC (Figure 2, *E*).

Both scaffolds had low degradation in 1 × PBS solution (data no shown), and low degradation in pH 5.5 physiological-like solution (Figure S2), with less than 8% weight loss after 4 weeks and no significant difference between GNP-CPC and CPC ($p > 0.05$). However, when immersed in pH 4 physiological-like solution, the degradation rates of the two scaffolds were different, with GNP-CPC degrading significantly faster ($p < 0.01$, Figure 2, *F*). In addition, gold released from GNP-CPC after immersing in 1× PBS for 4 weeks was detected; quantitative measurement by AAS showed that to be 0.61 ± 0.19 mg/L per scaffold. These results demonstrated that when immersed in culture media, GNPs could be slowly released from GNP-CPC.

Surface properties of GNP-CPC

The measurement of water contact angle is shown in Figure 3. The detection process is presented in Supplementary Video 1. CPC was detected first, followed by GNP-CPC. It shows that the angles are nearly 0 in both groups (Figure 3, *A* and *B*). Differences were found in water spreading areas. To observe the differences more clearly, neural red solution was used (Figure 3, *C* and *D*). The water drop spreading on GNP-CPC surface was larger in area than that on CPC (Figure 3, *E*, $p < 0.01$). The protein adsorption was significantly increased in GNP-CPC (Figure 3, *F*, $p < 0.01$), possibly due to the finer microstructure in GNP-CPC increasing the surface area compared with CPC control.

Biological properties of GNP-CPC

hDPSCs adhesion and spreading was examined at 4 h (Figure 4, *A*). While cells on CPC control had limited spread, cells on GNP-CPC had better spread and extended cytoskeletal processes. Cell spreading area was significantly greater on GNP-CPC than on CPC control (Figure 4, *B*, $p < 0.05$). The ratio of adhered cells after 4 h culturing was also higher on GNP-CPC than on CPC (Figure 4, *C*, $p < 0.01$). Cell proliferation of both groups was examined up to 14 days (Figure 4, *D*). Significant differences were detected at 14 days ($p < 0.05$). It was consistent with fluorescent cellular images, presenting as denser and thicker cell layers on GNP-CPC.

ALP activity was shown in Figure 5, *A*. Both groups saw a steady increase from day 4 to 7. A more obvious increase was from day 7 to 14. GNP-CPC showed significant higher ALP activities at day 7 and day 14 than CPC control ($p < 0.01$). The osteoblast-specific mRNA expressions, including ALP, COLIα, Runx2, and OCN genes, are plotted in Figure 5, *B* and *C*. GNP-CPC had higher expressions of ALP, COLIα and Runx2 genes at 7 days than CPC control ($p < 0.01$). However, the expression of OCN was similar between the two groups at 7 days ($p > 0.05$). At 14 days, higher levels of ALP, Runx2, and OCN genes were detected in GNP-CPC ($p < 0.01$). The OCN level was increased by about 4 folds.

Representative images of mineral synthesis by hDPSCs are shown in Figure 6, *A*. From 1 to 21 days, the red staining of synthesized bone mineral matrix covering the scaffolds became denser and darker red. The quantitative results are plotted in Figure 6, *B*. Cells on GNP-CPC had greater mineral synthesis than on CPC control at 14 days ($p < 0.05$); mineral synthesis by cells on GNP-CPC at 21 days was nearly 2-fold of that on CPC control.

GNPs internalized by co-cultured hDPSCs

TEM was done to detect the endocytosed GNPs by hDPSCs on GNP-CPC. The images showed that the nanostructured aggregates were taken up by the hDPSCs (Figure 7). The endocytotic aggregates were in perinuclear compartments and vesicular structures close to the cell nucleus. Most of the internalized aggregates were detected in cytosol, both in and out of the endosomal vesicles. To confirm that there were GNPs in these aggregates inside the cells, quantitative measurement of

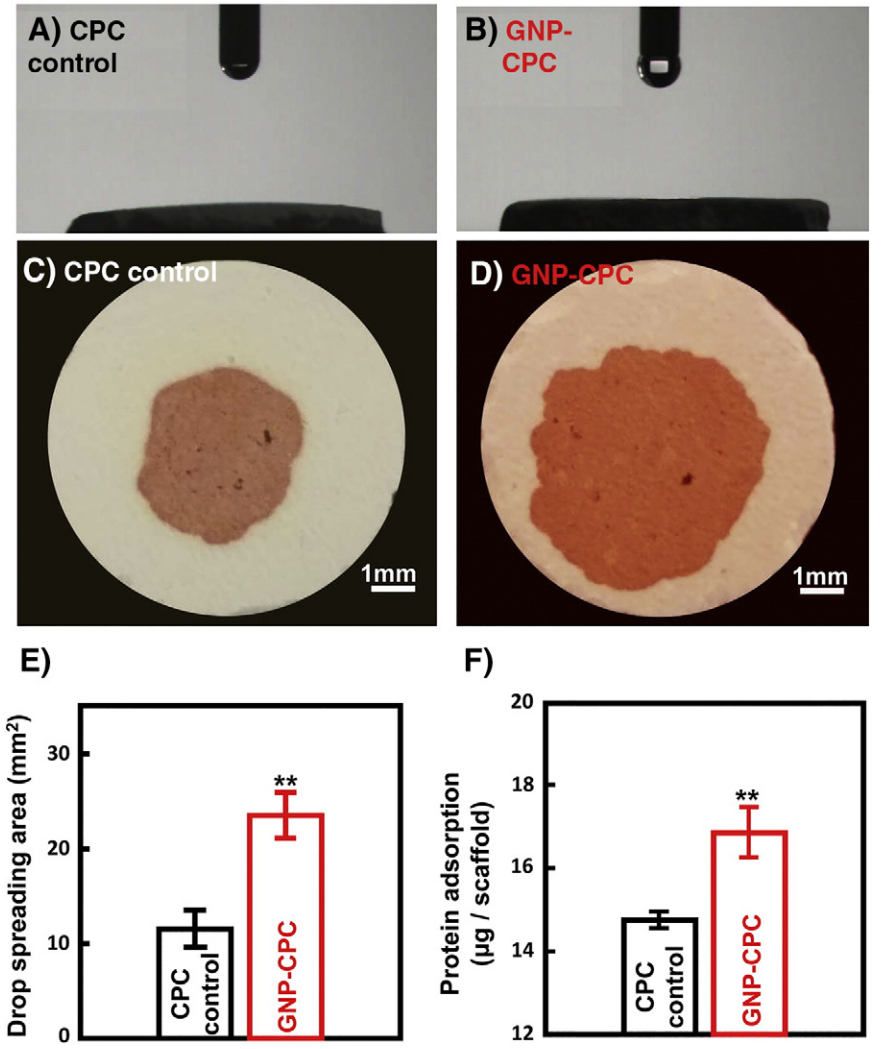

Figure 3. Surface properties of GNP-CPC and CPC. (A) and (B) Surface contact angles. (C) and (D) Images of drop spreading on the surfaces. (E) Measurements of drop spreading area. (n = 9). (F) Measurements of protein adsorption. (n = 9) (**, represents $p < 0.01$).

gold content inside the cells was performed via ICP-OES, yielding a gold content of 0.26 mg / g protein in the cells of the GNP-CPC group. In contrast, no gold was detected in the cells of the CPC control group. Therefore, the internalized aggregates contained GNPs. These aggregates could possibly be a mixture of both GNPs and CPC crystals.

Effects of GNPs on hDPSCs

To verify that GNPs can enhance hDPSCs functions whether there is a scaffold or not, hDPSCs were cultured in media containing 5 ppm GNPs without scaffolds. Cells cultured in media without GNPs served as control. Cell adhesion and spreading was tested, with no difference between media control and GNPs media (Figure S3, *A–C*). OD values of both groups were increased with time (Figure S3, *D*). Cell proliferation of hDPSCs cultured in GNPs media was greater than that of the control cells at 4 days ($p < 0.05$) and 7 days ($p < 0.01$). These results confirmed that GNPs indeed increased the proliferation of hDPSCs.

ALP staining results (Figure 8, *A*) demonstrated a denser staining in GNPs media than in media control. ALP activity amount per mg protein was significantly elevated over that of the control ($p < 0.01$, Figure 8, *B*). The expressions of osteogenic marker genes including ALP, Runx2, COLIα and OCN in hDPSCs were assayed by qRT-PCR at 14 days. Expressions of the above four marker genes in GNPs media were all up-regulated, compared with media control ($p < 0.01$, Figure 8, *C*). In addition, mineral synthesis by the cells was evaluated by ARS staining (Figure 8, *D*) at 14 days. Dark red staining was denser and thicker in GNPs media. Cells in GNPs media had significantly greater mineral synthesis than in media control ($p < 0.01$, Figure 8, *E*), achieving nearly a three-fold increase. These results indicated that GNPs could enhance bone matrix formation by hDPSCs.

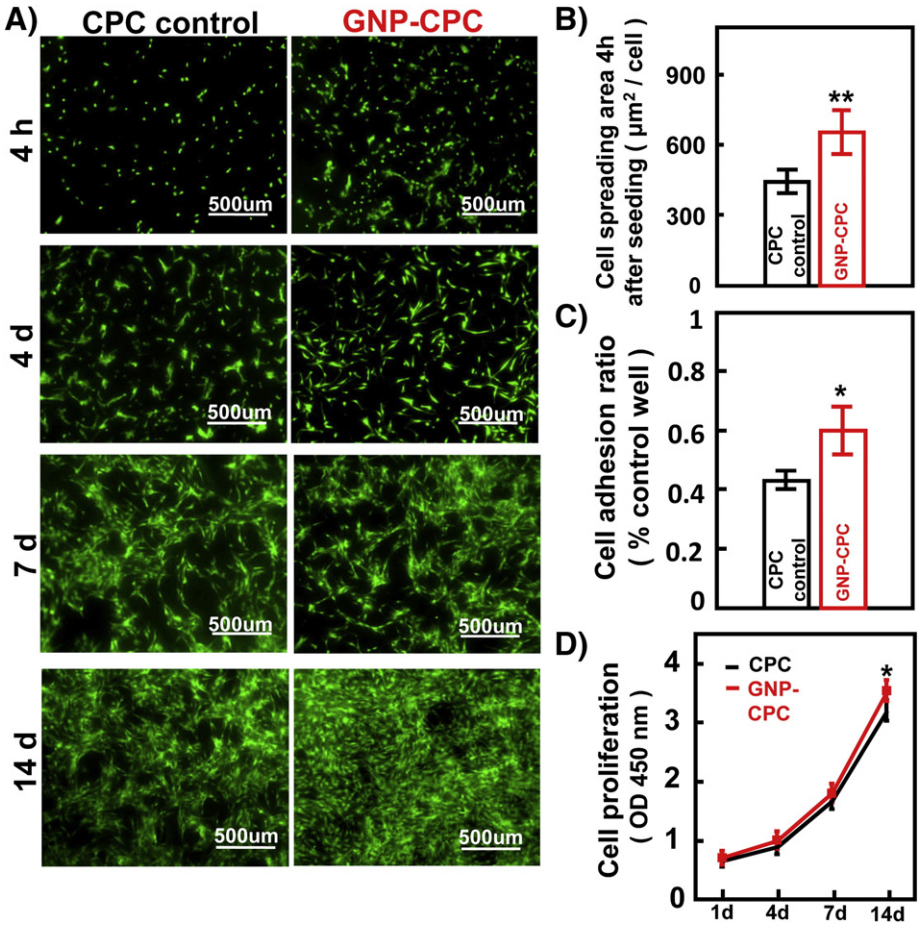

Figure 4. Cell adhesion and proliferation activities of GNP-CPC and CPC. (A) Live/Dead staining images of hDPSCs on the scaffolds at different time points. (B) Quantitative analysis of cell spreading area at 4 h after seeding. (n = 6). (C) Quantitative analysis of adhered cell ratio at 4 h after seeding. (n = 4). (D) hDPSCs were cultured on the scaffolds for 1, 4, 7, 14 days, and detected by CCK-8 assay. (n = 4). (*, represents $p < 0.05$; **, represents $p < 0.01$).

Discussion

The present study developed a novel GNP-CPC scaffold and greatly enhanced the osteogenic induction of hDPSCs on GNP-CPC for the first time. The hypotheses were proven that the addition of GNPs improve the properties of CPCs such as wetting and protein adsorption as well as cell attachment and spreading; that the osteogenic differentiation of hDPSCs were greatly improved via GNPs incorporation in CPCs, demonstrating substantial increases in ALP activity and osteogenic gene expressions, and a 2–3-fold increase in bone matrix mineral synthesis than those without GNPs. While further studies are needed, the enhancements in cell functions appeared to be related to a finer microstructure of GNP-CPC scaffold and the release and uptake of GNPs by the co-cultured cells.

GNPs were added to CPCs in liquid form in this study, which would be easier to achieve a homogeneous dispersion than adding powder GNPs. Highly hydrophilic and well dispersed GNP solution could permeate into CPC powder and wrap the micro-particles, thus affecting the dissolution and precipitation reactions.[38] The resulting finer microstructure in GNP-CPC would increase the surface area where protein molecules involved in the cellular adhesion could better adhere, achieving better cell spreading on GNP-CPC. The nanoscale surface topography of artificial materials plays a significant role in interactions with biological systems such as proteins and cells as it can resemble extracellular matrix (ECM) in which cells reside and interact.[39] The basement cell membrane in contact with the nano-structured surface could suffer tensile and relaxation mechanical forces that would rearrange its components and/or open ion channels to trigger cell behavior.[40] The other reason could be the protein adsorption. After contact of artificial material with a biological system, spontaneous adsorption of proteins onto the surface takes place. The resulting surface-bound protein layer, which is influenced by the geometrical, physical, and chemical surface properties of the biomaterial,[41] mediates the subsequent cell attachment through interactions with cell surface receptors. More protein adsorption can increase the cellular recognition sites and the adhesion processes,[41] and promote the overall cellular behaviors. Furthermore, the added GNPs could act as nanometer rollers between contacting CPC particles with the net effect of reducing

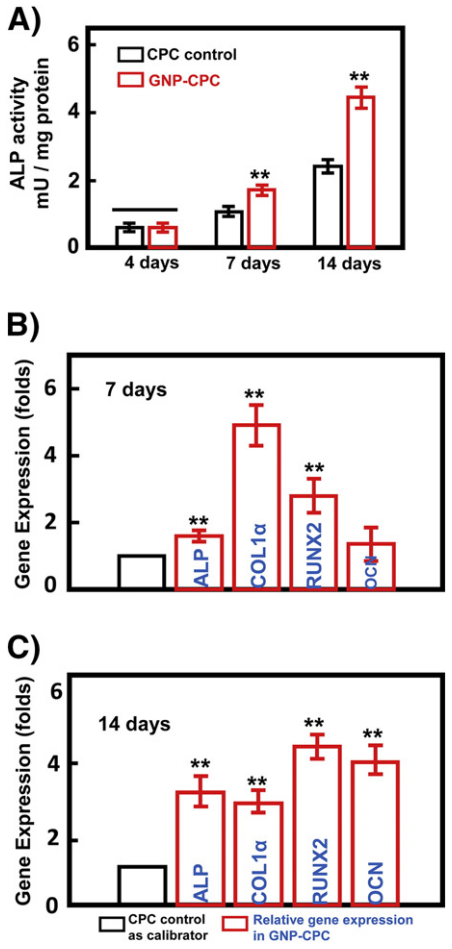

Figure 5. Osteogenic effects of GNP-CPC and CPC on hDPSCs. (A) ALP activity of the hDPSCs. ($n = 4$). (B) and (C) The expressions of ALP, COLIα, Runx2, and OCN genes of hDPSCs on the scaffolds after 7 days and 14 days culture ($n = 4$). (**, represents $p < 0.01$).

particle-particle interaction's friction.[38] This lubrication was possibly responsible for the faster degradation of GNP-CPC than CPC control.

The present study detected the existence of GNPs inside the hDPSCs seeded on GNP-CPC scaffolds to confirm the involvement of GNPs in enhancing cellular behavior. The existence of GNPs in GNP-CPC was not detectable by EDS and XRD. AAS was used to measure the gold content, to be 0.01 ± 0.001% by weight ratio, proving the existence of GNPs in GNP-CPC. GNP addition did not affect the conversion of the reactants to apatite phase according to XRD spectrum. When added into calcium phosphate ceramics, GNPs did not react with β-tricalcium phosphate and still presented as pure metal phase even after heat-treatment.[42] In this study, GNPs could be slowly released from GNP-CPC when immersed in physiological solution. Indeed, gold element was detected in the immersed solution of GNP-CPC. The released GNPs and CPC crystals were internalized by the seeded cells as confirmed via TEM. However, it should be noted that the cell microstructures could change due to the internalization of GNPs and CPC crystals. Further studies are needed to investigate the relationship between cell microstructure changes and the cell functions.

Furthermore, the present study verified the performance of cells cultured in GNPs media to detect the effects of GNPs alone on the cells without scaffold. The GNPs used were surface stabilized with citrate, negatively charged and well dispersed in the solution. Citrate-modified GNPs are the most commonly used; citrate as a stabilizing agent for GNPs is biologically inert and has no cytotoxic effects on different cell lines.[43] GNPs size, shape, surface charge and different surface chemical moieties can influence many cell behaviors particularly the uptake of the nanoparticles [44] as well as cytoskeletal remodeling.[45] Functional surface modification can further enhance the effects of GNPs.[46] GNPs enter cells through direct diffusion or endocytotic pathway.[47] Sphere-shaped nanoparticles are better for cellular uptake than rod or star shapes. Negatively-charged nanoparticles can be internalized by cells,[43] and is better than positively-charged ones regarding the nanoparticle endocytic process. They can prevent the cytotoxicity by the disruption of the cell membrane from direct diffusion.[47] The GNPs used here were spherical and hence suitable in size and shape for cellular uptake.[21,48] GNPs were reported to be internalized by several types of cells, including MSCs, ADSCs, and osteoblast cells, resulting in the osteogenic cell differentiation.[21,23,48] In addition, encapsulating DNA-functionalized gold nanoparticles into the intestinal stem cells were investigated for gene regulation therapy.[49] However, to date there has been no report on the effects of GNPs on hDPSCs.

For adding GNPs into the culture medium without scaffold, a concentration of 5 ppm was chosen because it was non-cytoxicitic.[50] Cell proliferation results indicated that the cells could tolerate the treatment of GNPs at this concentration, and induce a faster proliferation. The osteogenic differentiation was consistent with what was found in GNP-CPC. We measured the ALP activity at different time points in the GNPs alone on cells and in GNP-CPC. This was because a more direct effect to cells' ALP activity by adding GNPs into media was noticed as compared with adding GNPs into CPC in which the GNPs needed to be released from GNP-CPC first and then affected the cells. In addition, the released GNPs concentration in media of GNP-CPC group was lower than that of adding GNPs directly into media due to the repeated media change. Therefore, the ALP activity of the former was detected at an earlier time point than the later. No increase was found in cell adhesion and spreading via GNPs for cells attaching to TCPS. This may because that polystyrene surface was the same with or without GNPs in culture medium. This proved the point that for GNP-CPC scaffold, the enhanced cell attachment and spreading effect was from the microstructural changes (i.e., GNP-CPC scaffold had a finer microstructure than CPC control), not from the existence of GNPs in the medium.

In addition, the interaction between GNPs and cells was investigated because the physical and chemical properties of GNPs can strongly influence the biochemical properties of cells while they were in contact with each other. GNPs promoted cellular osteogenic differentiation by generating mechanical stresses on the cells from GNPs endocytosis through regulating the Yes-associated protein (YAP) activity.[51] The number of

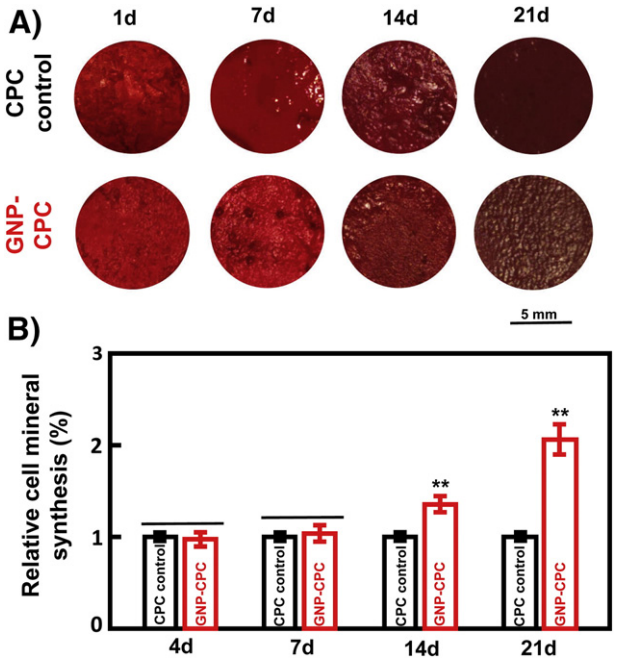

Figure 6. Alizarin red S (ARS) staining of GNP-CPC and CPC. (A) ARS staining images. (B) Quantitative analysis of mineral synthesis by the cells. ($n = 6$). (**, represents $p < 0.01$).

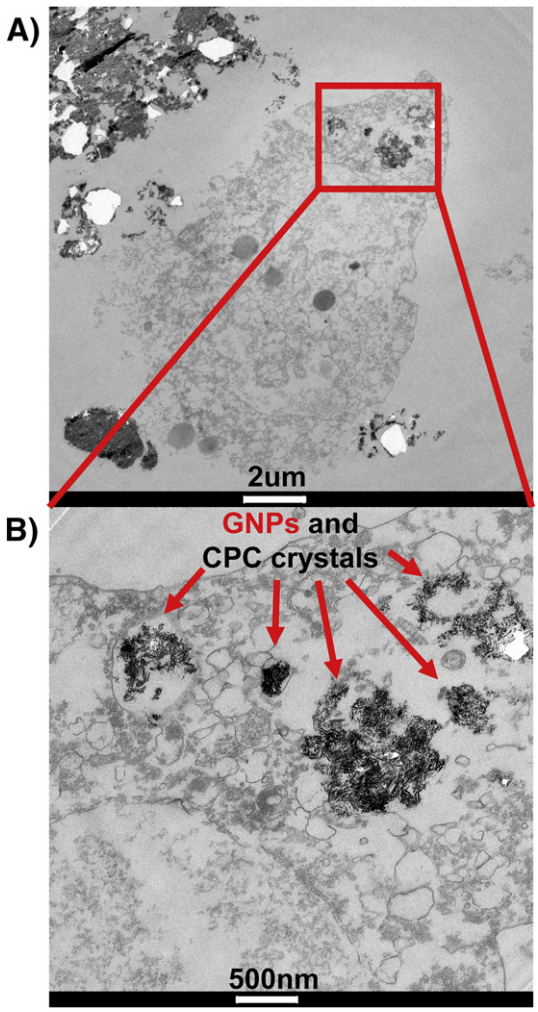

Figure 7. TEM images of hDPSCs after 7 days' culture on GNP-CPC.

GNPs uptake increased in a similar order as osteogenic differentiation.[52] GNPs interacted with the cell membranes and bind with proteins in the cytoplasm after GNPs internalization. The attached proteins around the GNPs as well as the internalized GNPs themselves could affect the osteogenic differentiation of the cells.[53] Yi CQ et al. used similar GNPs and found they promote osteogenic differentiation of mesenchymal stem cells through p38 MAPK pathway.[21] Furthermore, the increased osteopontin (OPN) expression on nanotopographical structures should be greater than the increase in OCN, due to the dual role of OPN as a protein containing the pro-adhesive tripeptide motif (RGD), and as a calcium sequestering component of the ECM.[54] Indeed, a significant increase in OPN expression was found (Figure S4), which was higher than the OCN expression in Figure 5, *C*.

Due to its active biological properties, GNPs are widely used to fabricate composite biomaterials. Poly(L-lactic acid) (PLLA) with GNPs were electrospun to create a scaffold for skeletal muscle repair.[55] In another study, gelatin-chitosan capped GNPs were shown to act as a matrix for the growth of HA crystals. This yielded a higher production of HA nanoparticles on the surface of gelatin-chitosan capped GNPs.[56] Aryal et al. showed that GNPs with collagen formed an efficient matrix for the growth of HA and the mineralized collagen showed potential for application in bone tissue repair and regeneration.[57] Furthermore, GNPs/HA-coated graphene composites demonstrated good potential for use as scaffold materials in bone regeneration.[58] However, the mechanism for the improved cellular behavior on these nanocomposites remains poorly understood and warrants further study.

In this study, we investigated GNP incorporation into CPC and the enhancement of osteogenesis of hDPSCs. The promising results indicate the potential of GNP incorporation into other types of calcium phosphate cements, as well as polymer-based[59] and hydrogel-based scaffolds[60,61] to enhance cell functions and tissue regeneration. In addition, other types of stem cells, including BMSCs, umbilical cord mesenchymal stem cells (hUCMSCs), embryonic stem cells and induced pluripotent stem cell-derived mesenchymal stem cells (hiPSC-MSCs) seeded on GNP-CPC scaffolds are also expected to have better cell functions and tissue regeneration via GNPs. Furthermore, the present study added GNPs using a water-based solution. Other forms of GNPs in various solutions, pastes, gels and powders can also be applied, requiring further investigation. Further studies are also needed to explore the cellular uptake pathway for GNPs, the intracellular trafficking process of GNPs, and the final fate of GNPs in the cells. In addition, in vivo tests are needed to determine the benefits on tissue regeneration and bone tissue engineering efficacy via GNPs in animal models.

In conclusion, a novel GNP-CPC scaffold was developed, and substantial enhancements in osteogenic differentiation of hDPSCs on GNP-CPC were obtained for the first time. The addition of GNPs improved the properties of CPC including

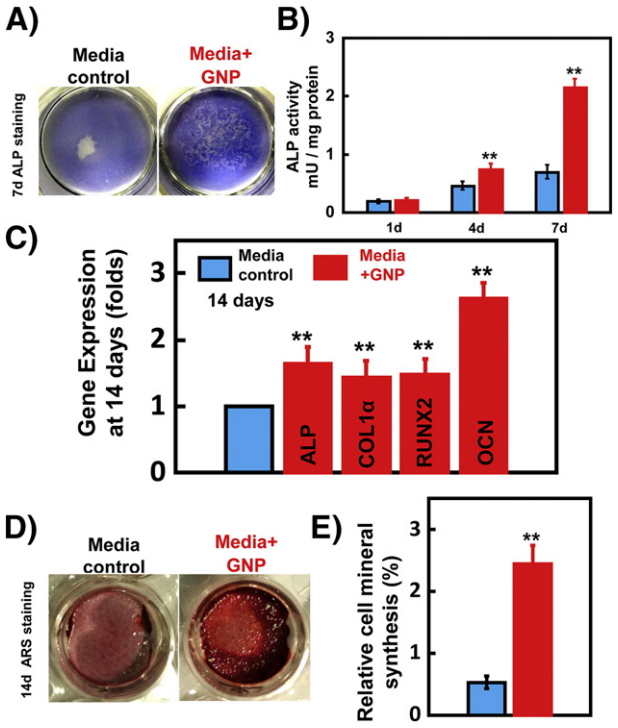

Figure 8. Osteogenic effects of GNPs on hDPSCs. (A) ALP staining of hDPSCs after 7 days culture in GNPs media. (B) ALP activity of the hDPSCs. (n = 4). (C) The expressions of ALP, COLIα, Runx2, and OCN genes of hDPSCs after 14 days culture (n = 4). (D) ARS staining images. (E) Quantitative analysis of mineral synthesis by the cells. (n = 6). (**, represents $p < 0.01$).

better wetting, greater protein adsorption, and improved cell attachment and spreading. The osteogenic differentiation of hDPSCs was markedly enhanced via GNP incorporation in CPC. Substantial increases in ALP activity and osteogenic gene expressions were achieved. The cellular bone matrix mineral synthesis was increased by 2–3 folds. The enhancement in cell functions was attributed to a finer microstructure of GNP-CPC scaffold and the release and cellular uptake of GNPs. Both the GNPs in culture medium and the GNPs incorporated into CPC scaffold enhanced the osteogenic differentiation of hDPSCs, showing great potential to improve bone regeneration.

Appendix A. Supplementary data

Supplementary data to this article can be found online at http://dx.doi.org/10.1016/j.nano.2017.08.014.

References

1. Johnson PC, Mikos AG, Fisher JP, Jansen JA. Strategic directions in tissue engineering. *Tissue Eng* 2007;**13**:2827-37.
2. Kaigler D, Krebsbach PH, Wang Z, West ER, Horger K, Mooney DJ. Transplanted endothelial cells enhance orthotopic bone regeneration. *J Dent Res* 2006;**85**:633-7.
3. Deville S, Saiz E, Nalla RK, Tomsia AP. Freezing as a path to build complex composites. *Science* 2006;**311**:515-8.
4. Ginebra MP, Espanol M, Montufar EB, Perez RA, Mestres G. New processing approaches in calcium phosphate cements and their applications in regenerative medicine. *Acta Biomater* 2010;**6**:2863-73.
5. Zhang J, Liu W, Schnitzler V, Tancret F, Bouler JM. Calcium phosphate cements for bone substitution: chemistry, handling and mechanical properties. *Acta Biomater* 2014;**10**:1035-49.
6. Bohner M, Gbureck U, Barralet JE. Technological issues for the development of more efficient calcium phosphate bone cements: a critical assessment. *Biomaterials* 2005;**26**:6423-9.
7. Chow LC. Next generation calcium phosphate-based biomaterials. *Dent Mater J* 2009;**28**:1-10.
8. O'Neill R, McCarthy HO, Montufar EB, Ginebra MP, Wilson DI, Lennon A, et al. Critical review: Injectability of calcium phosphate pastes and cements. *Acta Biomater* 2017;**50**:1-19.
9. Xu HH, Weir MD, Burguera EF, Fraser AM. Injectable and macroporous calcium phosphate cement scaffold. *Biomaterials* 2006;**27**:4279-87.
10. Zhao L, Weir MD, Xu HH. An injectable calcium phosphate-alginate hydrogel-umbilical cord mesenchymal stem cell paste for bone tissue engineering. *Biomaterials* 2010;**31**:6502-10.
11. Wang L, Zhang C, Li C, Weir MD, Wang P, Reynolds MA, et al. Injectable calcium phosphate with hydrogel fibers encapsulating induced pluripotent, dental pulp and bone marrow stem cells for bone repair. *Mater Biol Appl* 2016;**69**:1125-36.
12. Wang Q, Cheng H, Peng H, Zhou H, Li PY, Langer R. Non-genetic engineering of cells for drug delivery and cell-based therapy. *Adv Drug Deliv Rev* 2015;**91**:125-40.
13. Thein-Han W, Liu J, Xu HH. Calcium phosphate cement with biofunctional agents and stem cell seeding for dental and craniofacial bone repair. *Dent Mater* 2012;**28**:1059-70.
14. Ferreira LB, Bradaschia-Correa V, Moreira MM, Marques ND, Arana-Chavez VE. Evaluation of bone repair of critical size defects treated with simvastatin-loaded poly(lactic-co-glycolic acid) microspheres in rat calvaria. *J Biomater Appl* 2015;**29**:965-76.
15. Zhao L, Tang M, Weir MD, Detamore MS, Xu HH. Osteogenic media and rhBMP-2-induced differentiation of umbilical cord mesenchymal stem cells encapsulated in alginate microbeads and integrated in an injectable calcium phosphate-chitosan fibrous scaffold. *Tissue Eng Part A* 2011;**17**:969-79.
16. Fricain JC, Schlaubitz S, Le Visage C, Arnault I, Derkaoui SM, Siadous R, et al. A nano-hydroxyapatite--pullulan/dextran polysaccharide composite macroporous material for bone tissue engineering. *Biomaterials* 2013;**34**:2947-59.
17. Mohammadi M, Hesaraki S, Hafezi-Ardakani M. Investigation of biocompatible nanosized materials for development of strong calcium phosphate bone cement: comparison of nano-titania, nano-silicon carbide and amorphous nano-silica. *Ceram Int* 2014;**40**:8377-87.
18. Boisselier E, Astruc D. Gold nanoparticles in nanomedicine: preparations, imaging, diagnostics, therapies and toxicity. *Chem Soc Rev* 2009;**38**:1759-82.
19. Sperling RA, Rivera Gil P, Zhang F, Zanella M, Parak WJ. Biological applications of gold nanoparticles. *Chem Soc Rev* 2008;**37**:1896-908.
20. Dreaden EC, Alkilany AM, Huang X, Murphy CJ, El-Sayed MA. The golden age: gold nanoparticles for biomedicine. *Chem Soc Rev* 2012;**41**:2740-79.
21. Yi C, Liu D, Fong CC, Zhang J, Yang M. Gold nanoparticles promote osteogenic differentiation of mesenchymal stem cells through p38 MAPK pathway. *ACS Nano* 2010;**4**:6439-48.
22. Liu DD, Zhang JC, Yi CQ. Yang MS the effects of gold nanoparticles on the proliferation, differentiation, and mineralization function of MC3T3-E1 cells in vitro. *Chin Sci Bull* 2010;**55**:1013-9.
23. Choi SY, Song MS, Ryu PD, Lam AT, Joo SW, Lee SY. Gold nanoparticles promote osteogenic differentiation in human adipose-derived mesenchymal stem cells through the Wnt/β-catenin signaling pathway. *Nanomedicine* 2015;**10**:4383-92.

24. Sul OJ, Kim JC, Kyung TW, Kim HJ, Kim YY, Kim SH, et al. Gold nanoparticles inhibited the receptor activator of nuclear factor-κb ligand (RANKL)-induced osteoclast formation by acting as an antioxidant. *Biosci Biotechnol Biochem* 2010;**74**:2209-13.
25. Tsai SW, Liaw JW, Kao YC, Huang MY, Lee CY, Rau LR, et al. Internalized gold nanoparticles do not affect the osteogenesis and apoptosis of MG63 osteoblast-like cells: a quantitative, in vitro study. *PLoS One* 2013;**8**:e76545.
26. Discher DE, Mooney DJ, Zandstra PW. Growth factors, matrices, and forces combine and control stem cells. *Science* 2009;**324**:1673-7.
27. Gronthos S, Mankani M, Brahim J, Robey PG, Shi S. Postnatal human dental pulp stem cells (DPSCs) in vitro and in vivo. *S A* 2000;**97**:13625-30.
28. Tonomura A, Sumita Y, Ando Y, Iejima D, Kagami H, Honda MJ, et al. Differential inducibility of human and porcine dental pulp-derived cells into odontoblasts. *Connect Tissue Res* 2007;**48**:229-38.
29. Graziano A, d'Aquino R, Laino G, Papaccio G. Dental pulp stem cells: a promising tool for bone regeneration. *Stem Cell Rev* 2008;**4**:21-6.
30. Chamieh F, Collignon AM, Coyac BR, Lesieur J, Ribes S, Sadoine J, et al. Accelerated craniofacial bone regeneration through dense collagen gel scaffolds seeded with dental pulp stem cells. *Sci Rep* 2016;**6**:38814.
31. Wang P, Sun J, Lou Z, Fan F, Hu K, Sun Y, et al. Assembly-induced thermogenesis of gold nanoparticles in the presence of alternating magnetic field for controllable drug release of hydrogel. *Adv Mater* 2016;**28**:10801-8.
32. Sun L, Xu HH, Takagi S, Chow LC. Fast setting calcium phosphate cement-chitosan composite: mechanical properties and dissolution rates. *J Biomater Appl* 2007;**21**:299-315.
33. Costantino PD, Friedman CD, Jones K, Chow LC, Pelzer HJ, Sisson Sr GA. Hydroxyapatite cement. I. Basic chemistry and histologic properties. *Arch Otolaryngol Head Neck Surg* 1991;**117**:379-84.
34. He F, Li J, Ye J. Improvement of cell response of the poly(lactic-co-glycolic acid)/calcium phosphate cement composite scaffold with unidirectional pore structure by the surface immobilization of collagen via plasma treatment. *Biointerfaces* 2013;**103**:209-16.
35. Zhang N, Weir MD, Chen C, Melo MA, Bai Y, Xu HH. Orthodontic cement with protein-repellent and antibacterial properties and the release of calcium and phosphate ions. *J Dent* 2016;**50**:51-9.
36. Perez RA, Patel KD, Kim HW. Novel magnetic nanocomposite injectables: calcium phosphate cements impregnated with ultrafine magnetic nanoparticles for bone regeneration. *RSC Adv* 2015;**5**:13411-9.
37. Gregory CA, Gunn WG, Peister A, Prockop DJ. An alizarin red-based assay of mineralization by adherent cells in culture: comparison with cetylpyridinium chloride extraction. *Anal Biochem* 2004;**329**:77-84.
38. Vlad MD, del Valle LJ, Barracó M, Torres R, López J, Fernández E. Iron oxide nanoparticles significantly enhances the injectability of apatitic bone cement for vertebroplasty. *Spine* 2008;**33**:2290-8.
39. Lord MS, Foss M, Besenbacher F. Influence of nanoscale surface topography on protein adsorption and cellular response. *Nano Today* 2010;**5**:66-78.
40. Martínez E, Engel E, Planell JA, Samitier J. Effects of artificial micro- and nano-structured surfaces on cell behaviour. *Ann Anat* 2009;**191**:126-35.
41. Kasemo B. Biological surface science. *Surf Sci* 2002;**500**:656-77.
42. Bergmann C, Schwenke A, Sajti L, Chichkov B, Fischer H. Temperature-dependent morphology changes of noble metal tricalcium phosphate-nanocomposites. *Ceram Int* 2014;**40**:7931-9.
43. Freese C, Uboldi C, Gibson MI, Unger RE, Weksler BB, Romero IA, et al. Uptake and cytotoxicity of citrate-coated gold nanospheres: comparative studies on human endothelial and epithelial cells. *Part Fibre Toxicol* 2012;**9**:23.
44. Liu X, Huang N, Li H, Jin Q, Ji J. Surface and size effects on cell interaction of gold nanoparticles with both phagocytic and nonphagocytic cells. *Langmuir* 2013;**29**:9138-48.
45. Hoskins C, Cuschieri A, Wang L. The cytotoxicity of polycationic iron oxide nanoparticles: common endpoint assays and alternative approaches for improved understanding of cellular response mechanism. *J Nanobiotechnol* 2012;**10**:15.
46. Cao J, Wang R, Gao N, Li M, Tian X, Yang W, et al. A7RC Peptide modified paclitaxel liposomes dually target breast cancer. *Biomater Sci* 2015;**3**:1545-54.
47. Freese C, Gibson MI, Klok HA, Unger RE, Kirkpatrick CJ. Size- and coating-dependent uptake of polymer-coated gold nanoparticles in primary human dermal microvascular endothelial cells. *Biomacromolecules* 2012;**13**:1533-43.
48. Zhang D, Liu D, Zhang J, Fong C, Yang M. Gold nanoparticles stimulate differentiation and mineralization of primary osteoblasts through the ERK/MAPK signaling pathway. *Mater Sci Eng C* 2014;**42**:70-7.
49. Peng H, Wang C, Xu X, Yu C, Wang Q. An intestinal Trojan horse for gene delivery. *Nanoscale* 2015;**7**:4354-60.
50. Yu Q, Li J, Zhang Y, Wang Y, Liu L, Li M. Inhibition of gold nanoparticles (AuNPs) on pathogenic biofilm formation and invasion to host cells. *Sci Rep* 2016;**6**:26667.
51. Li J, Li JJ, Zhang J, Wang X, Kawazoe N, Chen G. Gold nanoparticle size and shape influence on osteogenesis of mesenchymal stem cells. *Nanoscale* 2016;**8**:7992-8007.
52. Mironava T, Hadjiargyrou M, Simon M, Rafailovich MH. Gold nanoparticles cellular toxicity and recovery: adipose derived stromal cells. *Nanotoxicology* 2014;**8**:189-201.
53. Mahmoudi M, Lynch I, Ejtehadi MR, Monopoli MP, Bombelli FB, Laurent S. Protein-nanoparticle interactions: opportunities and challenges. *Chem Rev* 2011;**111**:5610-37.
54. Yang J, McNamara LE, Gadegaard N, Alakpa EV, Burgess KV, Meek RM, et al. Nanotopographical induction of osteogenesis through adhesion, bone morphogenic protein cosignaling, and regulation of microRNAs. *ACS Nano* 2014;**8**:9941-53.
55. McKeon-Fischer KD, Freeman JW. Characterization of electrospun poly(L-lactide) and gold nanoparticle composite scaffolds for skeletal muscle tissue engineering. *J Tissue Eng Regen Med* 2011;**5**:560-8.
56. Sobhana SSL, Sundaraseelan J, Sekar S, Sastry TP, Mandal AB. Gelatin–chitosan composite capped gold nanoparticles: a matrix for the growth of hydroxyapatite. *J Nanoparticle Res* 2009;**11**:333-40.
57. Aryal S, Bhattarai SR, Prabu P, Kim HY. Immobilization of collagen on gold nanoparticles: preparation, characterization, and hydroxyapatite growth. *J Mater Chem* 2006;**16**:4642-8.
58. Crisan L, Crisan B, Soritau O, Baciut M, Biris AR, Baciut G, et al. In vitro study of biocompatibility of a graphene composite with gold nanoparticles and hydroxyapatite on human osteoblasts. *J Appl Toxicol* 2015;**35**:1200-10.
59. Peng HS, Liu XY, Wang GT, Li MH, Bratlie KM, Cochrana E, et al. Polymeric multifunctional Nanomaterials for Theranostics. *J Mater Chem B* 2015;**3**:6856-70.
60. Wang Q, Gu Z, Jamal S, Detamore MS, Berkland C. Hybrid hydroxyapatite nanoparticle colloidal gels are injectable fillers for bone tissue engineering. *Tissue Eng A* 2013;**35**:2586-93.
61. Wang Q, Jamal S, Detamore MS, Berkland C. PLGA-chitosan/PLGA-alginate nanoparticles blends as biodegradable colloidal gels for seeding human umbilical cord Mesenchymal stem cells. *J Biomed Mater Res A* 2011;**96A**:520-7.